Dynamic Interplay between Phase Separation and Wetting in a Binary Mixture Confined in a One-Dimensional Capillary

Hajime Tanaka

Department of Applied Physics and Applied Mechanics, Institute of Industrial Science, University of Tokyo, Minato-ku, Tokyo 106, Japan

(Received 9 October 1992)

Here we demonstrate that the phase separation of a binary mixture confined in a capillary is strongly affected by wetting phenomena for all the compositions. Near a symmetric composition, the hydrodynamics unique to a bicontinuous pattern leads to the extremely quick formation of a macroscopic wetting layer. Then this layer configuration becomes unstable because of the Rayleigh-like instability and eventually a stable, bamboolike structure is formed. This final structure is determined kinetically, but not thermodynamically. This is characteristic of a one-dimensional system with a conserved order parameter.

PACS numbers: 64.75.+g, 05.70.Fh, 64.60.−i, 68.45.Gd

Phase-separation phenomena have been extensively studied in the past two decades from both the fundamental and the practical viewpoints [1]. The essential features of phase separation in the bulk have already been understood to a considerable extent, and the pattern evolution dynamics can be well described by scaling theories or theories based on the time-dependent Ginzburg-Landau (TDGL) equation. However, an actual system used for any experiment always has a boundary, and thus the phase separation is under the influence of the surface to some extent. This surface effect, or the finite-size effect, plays a crucial role especially in a strongly confined geometry. Wetting phenomena near criticality were first studied by Cahn [2]. He predicted a complete wetting near criticality. In a stable region wetting phenomena can be discussed on the basis of energetics [2–7]. In metastable or unstable regions, on the other hand, since both wetting and phase separation are dynamic phenomena, we must go beyond energetics and study the dynamics. This dynamic interplay between phase separation and wetting has very recently attracted much attention [8–13], but this problem is still largely unexplored. In this Letter we report the first experimental study on the interplay between phase separation and wetting in a polymer solution confined in a semimacroscopic, capillary tube.

The samples used were mixtures of poly(vinyl methyl ether) (PVME) and water. The weight-average molecular weight of PVME was 98 200. In this mixture, a water-rich phase is more wettable to glass than a PVME-rich phase. The inner tube radius r_0 was varied in the range from 10 to 200 μm. Phase separation was triggered by a temperature jump from the stable, one-phase region to the unstable, two-phase region with a rate of 1.5°C/s. The temperature of the sample was changed by using a hot stage with a temperature controller (Linkam TH-600RMS). The phase separation process inside the capillary tube was observed by optical microscopy. We studied phase separation in a capillary also using other binary mixtures such as 2,6-lutidine/water mixtures and oligomer mixtures of styrene and ϵ-caprolactone. Among these mixtures the PVME/water mixture was found to be most appropriate for the present purpose because of the suitable coarsening dynamics, although the essential features were the same. In the very late stage, the pattern evolution is affected by gravity. However, in PVME/water mixtures the final phase-separated structure is formed before gravity starts to play a role.

Figure 1 shows the phase diagram for this mixture. This mixture has a lower-critical-solution-temperature-(LCST) type phase diagram. The symmetric composition is located around 7 wt% PVME, and weakly dependent on the quench depth because of the asymmetric shape of the phase diagram. Near the symmetric composition a bicontinuous, phase-separated structure appears at least in the initial stage. This percolation region is schematically shown in Fig. 1 as the shaded region.

Here we show the pattern evolution inside a capillary tube observed by optical microscopy. Figures 2(a) and 2(b) show the pattern evolution in a capillary tube for PVME/water (3/97) at $T=34.0$°C and for PVME/water (5/95) at $T=33.9$°C, respectively. In both cases, a PVME-rich phase which is less wettable to glass appears as droplets and the matrix wets the wall. Because of a

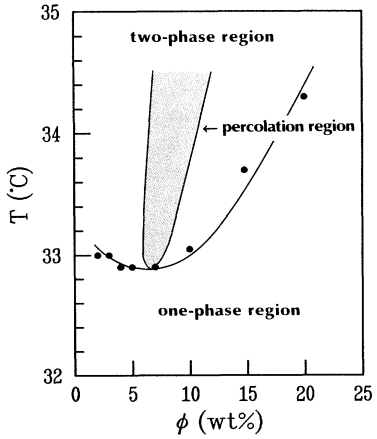

FIG. 1. Phase diagram of the PVME/water mixture.

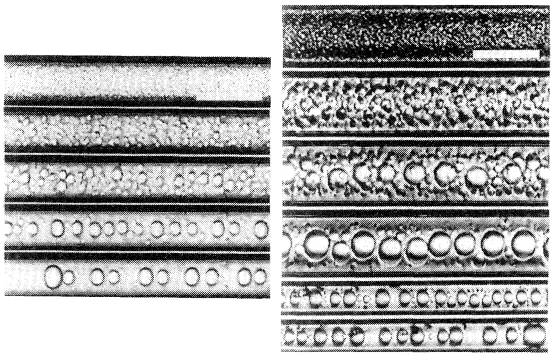

(a) (b)

FIG. 2. (a) Capillary phase separation in PVME/water (3/97). Photographs correspond to 5.0, 60.0, 120.0, 240.0, and 360.0 s after the temperature jump from 32.5 to 34.0 °C, respectively, from top to bottom. The bar corresponds to 80 μm. (b) Capillary phase separation in PVME/water (5/95). Photographs correspond to 10.0, 180.0, 300.0, 510.0, 660.0, and 2520 s after the temperature jump from 32.5 to 33.9 °C, respectively, from top to bottom. The bar corresponds to 80 μm for the top four photographs and to 200 μm for the bottom two photographs.

symmetry requirement, droplets eventually locate around the symmetrical axis of the capillary.

Figure 3 shows the pattern evolution in a capillary tube for PVME/water (7/93) at $T=33.5$°C. Here we see the very rapid formation of a wetting layer and the subsequent, Rayleigh-like instability [9,14–17], which transforms the tube configuration of the wetting layer into stable, periodic bridges. The formation of the wetting layer with smooth surface is accomplished within an extremely short time (~7 s). Macroscopic phase separation in this time scale is very unusual for a polymer solution.

Figures 4(a) and 4(b) show the pattern evolution in a capillary tube for PVME/water (10/90) at $T=33.1$ and 33.5°C, respectively. In both cases, the minority phase is water rich and droplets wet the inner glass surface. The wetting layer is slowly formed by the collision of droplets with the wall. It should be noted that this mechanism of wetting layer formation is different from that in Fig. 3. In Fig. 4(a), a stable wetting layer is eventually formed. In Fig. 4(b), on the other hand, the wetting layer becomes unstable and forms stable, periodic bridges, namely, a bamboolike structure.

First we discuss the above composition dependence of the pattern evolution. The pattern evolution in a 1D capillary can be classified into the following three cases: (1) $\phi_\alpha \gg \frac{1}{2}$ [ϕ_α and ϕ_β are the volume fractions of the more wettable (water-rich) and the less wettable (PVME-rich) phases, respectively], (2) $\phi_\alpha \sim \frac{1}{2}$ (the shaded region in Fig. 1), and (3) $\phi_\alpha \ll \frac{1}{2}$. The boundaries between the three regions are likely determined by percolation thresholds, namely, whether a bicontinuous, phase-separated structure appears in the initial stage or not (see Fig. 1). Figures 2(a) and 2(b) correspond to case (1), Fig. 3 corresponds to case (2), and Figs. 4(a) and 4(b) correspond to case (3).

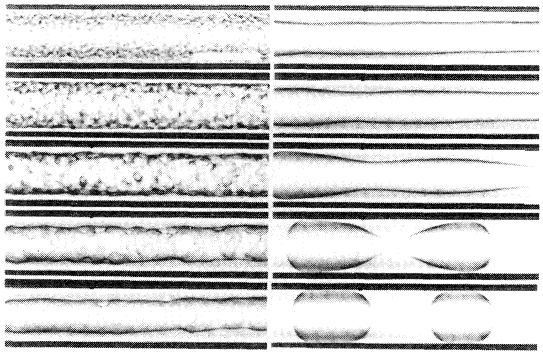

FIG. 3. Capillary phase separation in PVME/water (7/93). Photographs correspond to 4.0, 4.5, 5.0, 6.0, 7.0 (left column), 20.0, 60.0, 90.0, 130.0, and 150.0 s (right column) after the temperature jump from 32.5 to 33.5°C, respectively, from top to bottom. The bar corresponds to 200 μm.

When the minority phase is nonwettable to the glass [case (1)], droplets slowly coarsen by the Brownian coagulation and the evaporation-condensation mechanisms [1]. Since the van der Waals interaction between a droplet and the wall is roughly proportional to R/D (R the droplet radius, and D the distance between droplet surface and wall) [18], larger droplets feel a stronger repulsive interaction from the wall than smaller ones.

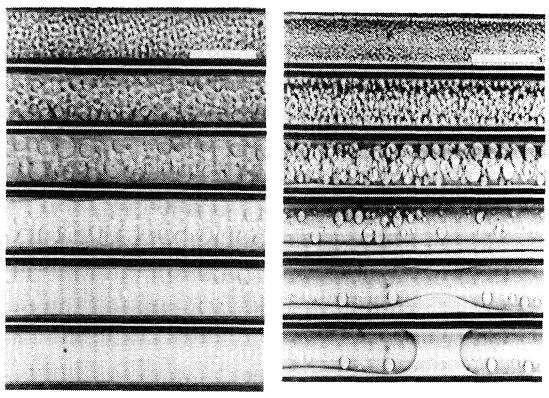

(a) (b)

FIG. 4. (a) Capillary phase separation in PVME/water (10/90). Photographs correspond to 30.0, 120.0, 240.0, 300.0, 420.0, and 1020.0 s after the temperature jump from 32.5 to 33.1°C, respectively, from top to bottom. The bar corresponds to 80 μm. (b) Capillary phase separation in PVME/water (10/90). Photographs correspond to 30.0, 180.0, 300.0, 480.0, 900.0, and 960.0 s after the temperature jump from 32.5 to 33.5°C, respectively, from top to bottom. The bar corresponds to 200 μm.

This interaction likely exceeds the thermal energy k_BT (k_B is Boltzmann's constant) for a large value of R/D. Thus larger droplets locate around the cylindrical axis at a higher probability because of a symmetry requirement. This weak, spatial confinement effect increases the chance of collision especially between large droplets and thus accelerates the coarsening. Such behavior is actually observed in Figs. 2(a) and 2(b). The droplet size finally exceeds the pore size [the crossover from three dimensions (3D) to one dimension (1D)], and the droplets transform into capsules [19].

When the minority phase forming droplets is more wettable to the glass [case (3)], the droplets are attracted to the wall by the van der Waals interaction. Thus the droplets gradually wet the glass and form the wetting layer. This wetting layer is stable for a shallow quench, while it is unstable for a deep quench and eventually breaks up into bridges by the Rayleigh instability. Since the more wettable phase feels the attractive interaction only from the wall, a layer configuration is first formed in either case. It is shown that in a 1D capillary the transition between tube and plug configurations occur at $\phi_\beta=\phi_t=(\sigma/\Delta\gamma)^2$, where σ is the interfacial tension between the two phases and $\Delta\gamma$ is the difference in the wettability to the wall between the two phases, provided that an effective interfacial potential in Ref. [9] is weak for a semimacroscopic capillary. Since $\sigma=\sigma_0\epsilon^\mu$ ($\mu=1.26$) and $\Delta\gamma=\Delta\gamma_0\epsilon^\delta$ ($\delta=0.34$), where $\epsilon=(T-T_c)/T_c$ [1], $\phi_t=(\sigma_0/\Delta\gamma_0)^2\epsilon^{2(\mu-\delta)}$ under the constraint that $\frac{1}{2}<\phi_t<1$. Thus, for $\phi_\beta>\phi_t$ (for a shallow quench) complete wetting is favored, while for $\phi_\beta\leq\phi_t$ (for a deep quench) partial wetting is favored. Hydrodynamic stability analysis [17] also indicates the layer or unduloid configuration is stable for a thinner film, namely, for a larger value of ϕ_β. These predictions are consistent with the results for PVME/water (10/90).

When the composition is close to the symmetrical one [case (2)], bicontinuous phase separation occurs. In this particular phase-separated structure, the hydrodynamics unique to the bicontinuous tube morphology [10,20] plays a drastic role under the influence of the wetting effect. The more wettable phase can be continuously supplied into the wetting layer through the percolated tubes by this hydrodynamic flow. This causes the extremely quick formation of the wetting layer. The thickness of this wetting layer d_w likely grows as $d_w\sim(\sigma/\eta)t$ in the initial stage. This is because the total flux into the wetting layer through bicontinuous tubes (radius a) per area (S), Q_t, is proportional to (flux per tube $\times$ number of tubes) $=[\sim(\sigma/\eta)a^2]\times(\sim S/a^2)$ and $S(d/dt)d_w$ should be proportional to Q_t. This linear growth of d_w has been experimentally confirmed [21]. It should be noted that the growth dynamics of the wetting layer is not affected by the wettability ($\Delta\gamma$) after the wall surface is completely covered by the more wettable phase.

Here we briefly discuss the dynamics of the wetting layer formation. Table I shows the ratio of the time required to form the wetting layer (τ_w) to the final layer thickness (d_w^f) just before the instability, τ_w/d_w^f, for various quench conditions. The difference in τ_w between the capillaries having different pore sizes is found to scale as τ_w/d_w^f. This is consistent with the above prediction. The difference in τ_w between the bicontinuous and the droplet morphologies is more than the 2 orders of magnitude. This reflects the difference in the mechanism of the layer formation. The small value of τ_w for 10 wt% PVME at $T=34.1$°C is explained by the fact that under the deep quench condition bicontinuous phase separation appears even at this composition (see Fig. 1). For bicontinuous phase separation, τ_w/d_w^f should be proportional to η/σ from the above argument. The dependence of τ_w/d_w^f on the quench depth ϵ for a PVME/water (7/93) mixture is consistent with an increase in σ ($\sigma\propto\epsilon^\mu$) and a slight decrease in η with increasing ϵ.

TABLE I. The formation time of a wetting layer.

No.	ϕ_p[a] (wt%)	T (°C)	r_0 (μm)	Type	τ_w (s)	τ_w/d_w^f (s/μm)
E7-1	7	33.2	70.5	bi[b]	4.1	0.14
E7-2	7	33.2	28.2	bi	1.2	0.13
E7-3	7	33.4	98.7	bi	4.4	0.12
E7-4	7	33.5	81.8	bi	4.0	0.11
E7-5	7	33.5	28.2	bi	1.3	0.11
E7-6	7	33.6	49.4	bi	1.4	0.08
E7-7	7	33.7	51.0	bi	1.4	0.09
E7-8	7	34.0	70.5	bi	1.8	0.04
E10-1	10	33.3	36.0	dr[c]	420	···
E10-2	10	33.6	71.8	dr	480	···
E10-3	10	33.6	66.2	dr	210	···
E10-4	10	34.1	42.5	bi	1.4	0.11

[a]PVME concentration. [b]Bicontinuous. [c]Droplet.

Next we analyze the dynamics of bridge formation near the symmetric composition. This phenomenon is known as Rayleigh-like instability for a capillary [9,14–17]. For a quantitative analysis of the bridge formation, the minimum radius of the deforming tube of the β phase, r_m, is measured as a function of time $\Delta t=t_c-t$, where t_c is the time of the bridge formation and t is the time. Figure 5 shows a scaling plot for the relation be-

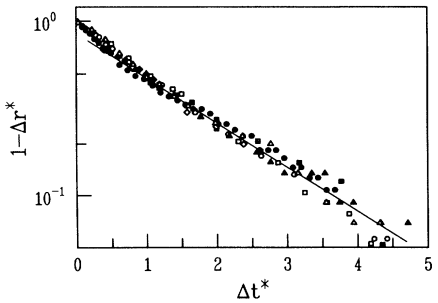

FIG. 5. Plot of $1-\Delta r^*$ against Δt^*. E7-1, ○ and ●; E7-2, ◆; E7-3, □; E7-4, ■; E7-7, △ and ▲; E7-8, ◇.

tween Δr^* ($=r_m/r_i$, with r_i the initial tube radius before deformation, namely, just after the formation of the wetting layer) and Δt^* [$=\Delta t/\Delta t_{1/2}$, with $\Delta t_{1/2}$ experimentally determined by $\Delta r^*(\Delta t_{1/2}) = \frac{1}{2}$]. In the initial stage (for a large Δr^*) the fluctuation $1-\Delta r^*$ grows exponentially as predicted by the theories [15–17], while in the late stage (for a small Δr^*) it starts to deviate from the exponential growth because of nonlinear contributions. Eventually, Δr^* has a linear dependence on Δt^* in the late stage [21], which can be explained by the simple hydrodynamics unique to a tube configuration based on the Poiseuille flow. The growth dynamics of fluctuation coming from the Rayleigh-like instability can be scaled by the characteristic growth speed ($\Delta t_{1/2}$), and can be described by the universal function near the symmetric composition (see Fig. 5). The evolution dynamics is governed by the balance between surface-tension driving forces and viscous resistance in the outer fluid. Thus the initial exponential growth of the instability is characterized by the time constant τ, which is proportional to $(\eta r_i/\sigma)h(r_i/r_0)$ [15–17], where $h(r_i/r_0)$ is a complex function of r_i/r_0 and other variables [17], namely, $\Delta t_{1/2} \propto (\eta r_i/\sigma)h(r_i/r_0)$. This relation is qualitatively consistent with the observed dependence of $\Delta t_{1/2}$ on the quench depth, although an analysis including $h(r_i/r_0)$ is necessary for a detailed comparison.

In a 1D capillary, the system stops coarsening in the late stage even though it does not reach the lowest energy state. The final bridge structure of the phase separation is determined kinetically by the fastest growing mode, and not thermodynamically. The characteristic size of the bridge ($\lambda_{\max}$) is roughly given by $\sim 2\pi r_i$ according to the classical theories on the Rayleigh instability [15–17]. This length scale appears because the lobes must be axially symmetrical constant-pressure surfaces. As predicted by Liu *et al.* [9], after the formation of the bamboolike structure the coarsening is extremely slow, since the evaporation-condensation mechanism plays a minor role in the coarsening because of the absence of a curvature difference between plugs. This is because the only relevant length scale is the radius of the capillary tube (r_0) after the crossover from 3D to 1D. Further, thermal motion of the bridge structure is not allowed from the conservation law because of the 1D nature. Thus the bamboolike structure is likely stable or metastable and no coarsening is expected in the late stage. It is characteristic of a 1D system having a conserved order parameter that the kinetics instead of the energetics dominates the final structure.

In summary, we have found that in a 1D capillary the phase-separation behavior is strongly affected by wetting phenomena for all the compositions, although the manner of coupling between the two phenomena is strongly dependent on the composition. This is a specific feature of a 1D system coming from a strong, geometrical confinement. In a 2D system, on the other hand, phase separation is strongly coupled with wetting only when the minority phase is more wettable to the walls [21]. The behavior described here should be universal for any binary mixture confined in a semimacroscopic, capillary tube. Since the wetting phenomena so drastically affect phase-separation behavior even in a semimacroscopic container, special care should be taken to study bulk phase separation experimentally.

This work was partly supported by a Grant-in-Aid from the Ministry of Education, Science, and Culture, Japan, by a grant from Kanagawa Academy of Science and Technology, and by a grant from Iketani Science and Technology Foundation.

[1] J. D. Gunton, M. San Miguel, and P. Sahni, in *Phase Transitions and Critical Phenomena*, edited by C. Domb and J. H. Lebowitz (Academic, London, 1983).
[2] J. W. Cahn, J. Chem. Phys. **66**, 3667 (1977).
[3] D. Jasnow, Rep. Prog. Phys. **47**, 1059 (1984).
[4] P. G. de Gennes, Rev. Mod. Phys. **57**, 827 (1985).
[5] R. Moldover and J. W. Cahn, Science **207**, 1073 (1980).
[6] D. W. Pohl and W. I. Goldberg, Phys. Rev. Lett. **48**, 185 (1982).
[7] D. Beysens and D. Esteve, Phys. Rev. Lett. **54**, 2123 (1985).
[8] K. Williams and R. A. Dawe, J. Colloid Interface Sci. **117**, 81 (1987).
[9] A. J. Liu, D. J. Durian, E. Herbolzheimer, and S. A. Safran, Phys. Rev. Lett. **65**, 1897 (1990).
[10] P. Guenoun, D. Beysens, and M. Robert, Phys. Rev. Lett. **65**, 2406 (1990).
[11] R. A. L. Jones, L. J. Norton, E. J. Kramer, F. S. Bates, and P. Wilzius, Phys. Rev. Lett. **66**, 1326 (1991).
[12] P. Wiltzius and A. Cumming, Phys. Rev. Lett. **66**, 3000 (1991).
[13] F. Bruder and R. Brenn, Phys. Rev. Lett. **69**, 624 (1992).
[14] L. Rayleigh, Philos. Mag. **34**, 145 (1982).
[15] S. L. Goren, J. Fluid Mech. **12**, 309 (1962).
[16] P. S. Hammond, J. Fluid Mech. **137**, 363 (1983).
[17] M. Johnson, R. D. Kamm, L. W. Ho, A. Shapiro, and T. J. Pedley, J. Fluid Mech. **233**, 141 (1991).
[18] J. N. Israerachivili, *Intermolecular and Surface Forces* (Academic, New York, 1985).
[19] On the notations of "capsule," tube," and "plug," see Ref. [10].
[20] E. D. Siggia, Phys. Rev. A **20**, 595 (1979).
[21] H. Tanaka (unpublished).

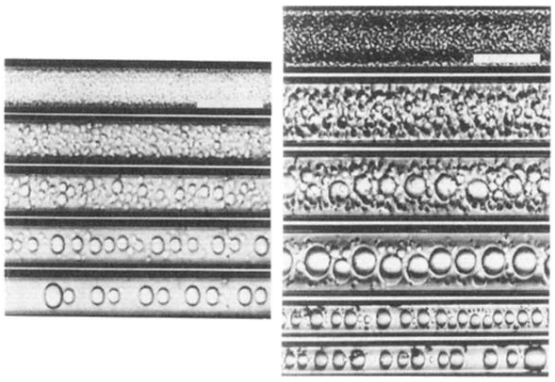

(a) (b)

FIG. 2. (a) Capillary phase separation in PVME/water (3/97). Photographs correspond to 5.0, 60.0, 120.0, 240.0, and 360.0 s after the temperature jump from 32.5 to 34.0 °C, respectively, from top to bottom. The bar corresponds to 80 μm. (b) Capillary phase separation in PVME/water (5/95). Photographs correspond to 10.0, 180.0, 300.0, 510.0, 660.0, and 2520 s after the temperature jump from 32.5 to 33.9 °C, respectively, from top to bottom. The bar corresponds to 80 μm for the top four photographs and to 200 μm for the bottom two photographs.

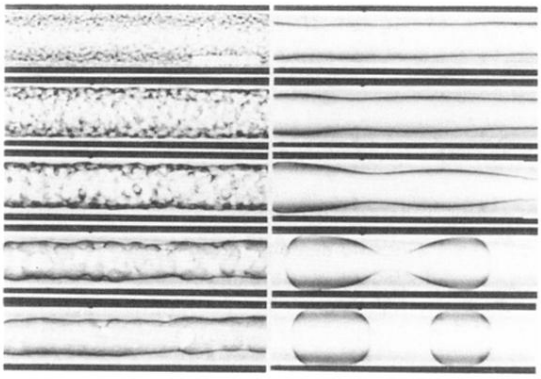

FIG. 3. Capillary phase separation in PVME/water (7/93). Photographs correspond to 4.0, 4.5, 5.0, 6.0, 7.0 (left column), 20.0, 60.0, 90.0, 130.0, and 150.0 s (right column) after the temperature jump from 32.5 to 33.5°C, respectively, from top to bottom. The bar corresponds to 200 μm.

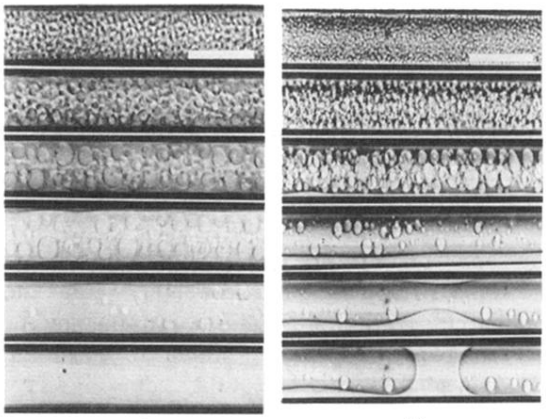

(a) (b)

FIG. 4. (a) Capillary phase separation in PVME/water (10/90). Photographs correspond to 30.0, 120.0, 240.0, 300.0, 420.0, and 1020.0 s after the temperature jump from 32.5 to 33.1°C, respectively, from top to bottom. The bar corresponds to 80 μm. (b) Capillary phase separation in PVME/water (10/90). Photographs correspond to 30.0, 180.0, 300.0, 480.0, 900.0, and 960.0 s after the temperature jump from 32.5 to 33.5°C, respectively, from top to bottom. The bar corresponds to 200 μm.